Int J Thermophys (2009) 30:1001–1013
DOI 10.1007/s10765-009-0573-7

A Comparative Performance Analysis and Optimization of the Irreversible Atkinson Cycle Under Maximum Power Density and Maximum Power Conditions

Yasin Ust

Received: 17 December 2008 / Accepted: 5 March 2009 / Published online: 1 April 2009

Abstract This article reports the thermodynamic optimization based on the maximum power (MP) and maximum power density (MPD) criteria for an irreversible Atkinson heat-engine model which includes internal irreversibility resulting from the adiabatic processes. The power density, power output, and thermal efficiency are obtained by introducing the isentropic temperature ratio of the compression process, cycle temperature ratio, and the compression and expansion efficiencies. Optimal performance and design parameters of the Atkinson cycle are obtained analytically for the MP conditions and numerically for the MPD conditions. The results at MPD conditions are compared with those results obtained by using the MP and maximum thermal efficiency criteria. The effects of the cycle temperature ratio and irreversibilities on the general and optimal performances are investigated. It is shown that for the Atkinson cycle, a design based on the MPD conditions is more advantageous from the point of view of engine sizes and thermal efficiency.

Keywords Atkinson heat-engine · Maximum power density · Optimal performance · Performance analysis · Thermodynamic optimization

List of symbols

C_P Heat capacity at constant pressure ($\mathrm{kJ \cdot kg^{-1} \cdot K^{-1}}$)
C_V Heat capacity at constant volume ($\mathrm{kJ \cdot kg^{-1} \cdot K^{-1}}$)
k Ratio of the specific heat capacities $= (C_P/C_V)$
$\dot{m}$ Cycle mass times the number of cycles per second ($\mathrm{kg \cdot s^{-1}}$)

Y. Ust (✉)
Department of Naval Architecture and Marine Engineering,
Yildiz Technical University,
Besiktas 34349, Istanbul, Turkey
e-mail: yust@yildiz.edu.tr

MP Maximum power
MPD Maximum power density
P Pressure (kPa)
$\dot{Q}$ Rate of heat transfer (kW)
S Entropy ($kJ \cdot K^{-1}$)
T Temperature (K)
V Volume (m^3)
$\dot{W}$ Power output (kW)
$\dot{W}_d$ Power density (kPa)

Greek letters

α Cycle temperature ratio $= T_3/T_1$
ϕ Isentropic temperature ratio of the compression process $= T_{2S}/T_1$
η Thermal efficiency
η_C Compression efficiency
η_E Expansion efficiency

Subscripts

C Compression
d Density
E Expansion
max Maximum
mef Maximum thermal efficiency conditions
mp Maximum power conditions
mpd Maximum power density conditions

Superscripts

– Dimensionless

1 Introduction

The Atkinson cycle engine is a type of internal combustion engine invented by James Atkinson in 1882. The Atkinson cycle is designed to provide efficiency at the expense of power. The Atkinson cycle allows the intake, compression, power, and exhaust strokes of the four-stroke cycle to occur in a single turn of the crankshaft. Owing to the linkage, the expansion ratio is greater than the compression ratio, leading to greater efficiency than with engines using the alternative Otto cycle. The Atkinson cycle may also refer to a four-stroke engine in which the intake valve is held open longer than normal to allow a reverse flow of intake air into the intake manifold. This reduces the effective compression ratio and, when combined with an increased stroke and/or reduced combustion chamber volume, allows the expansion ratio to exceed the compression ratio while retaining a normal compression pressure. This is

desirable for improved fuel economy because the compression ratio in a spark ignition engine is limited by the octane rating of the fuel used. A high expansion ratio delivers a longer power stroke, allowing more expansion of the combustion gases and reducing the amount of heat wasted in the exhaust. This makes for a more efficient engine [1].

Identifying the performance limits of thermal systems and optimizing thermodynamic processes and cycles including finite-time, finite-rate, and finite-size constraints has been the subject of many thermodynamic modeling and optimization studies in physics and engineering literature [2–7]. In recent years, there have been many performance analyses for the Atkinson heat engine based on reversible, endo-reversible, and irreversible cycle models by using different objective functions such as the work output, power output, efficiency, etc. [8–20]. The performance analyses based on the above optimization criteria do not take the effect of engine sizes related to the investment cost into account. In order to include the effects of engine size in the performance analysis, Sahin et al. [21,22] introduced a new optimization criterion called the maximum power density (MPD) analysis. Using the MPD criterion, they investigated optimal performance conditions for reversible [21] and irreversible [22] non-regenerative Joule-Brayton heat engines. In their study, they maximized the power density (the ratio of power to the maximum specific volume in the cycle) and found design parameters at MPD conditions which lead to smaller and more efficient Joule-Brayton engines than those engines working at maximum power (MP) conditions. Many authors then applied the MPD technique to different heat-engine models [23–33].

The MPD technique has also been applied to the Atkinson cycle by Chen et al. [34] and Wang and Hou [35]. A power density maximization of a reversible Atkinson cycle has been performed by Chen et al. [34]. Their results showed that the efficiency at MPD is always greater than that at MP, and the design parameters at MPD lead to smaller and more efficient Atkinson engines with larger pressure ratios. Performance analysis and a comparison of an Atkinson cycle coupled to variable temperature heat reservoirs under MP and MPD conditions have been done by Wang and Hou [35]. The Atkinson cycle was internally reversible but externally irreversible, since there was external irreversibility of heat transfer during the processes of constant volume heat addition and constant pressure heat rejection. The results showed that an engine design based on MPD with constant effectiveness of the hot- and cold-side heat exchangers or constant inlet temperature ratio of the heat reservoirs will have smaller size but higher efficiency, compression ratio, expansion ratio, and maximum temperature than the one based on MP.

In this article, the MPD performance analysis performed by Chen et al. [34] and Wang and Hou [35] for the reversible and endo-reversible Atkinson heat-engine model is extended to an irreversible Atkinson heat-engine model by considering internal irreversibility effects. In this context, the optimal performance and design parameters under MPD conditions are investigated. The results are comparatively discussed with respect to the results obtained by using the MP and maximum thermal efficiency criteria. In addition, the effects of cycle temperature ratio and the internal irreversibilities resulting from the adiabatic processes on the performance will also be examined.

2 Performance Optimization for an Irreversible Atkinson Cycle

P-V and *T-S* diagrams of an standard irreversible Atkinson cycle with air is shown in Fig. 1. In the *T-S* diagram, the process 1–2s is an isentropic compression, while the process 1–2 takes into account internal irreversibilities. The heat addition occurs in the constant volume process 2–3. Process 3–4s is an isentropic expansion, while the process 3–4 takes into account internal irreversibilities. A constant pressure heat rejection process, 4–1, completes the cycle. The heat added to the working fluid during the process $2 \rightarrow 3$ is

$$\dot{Q}_{\text{in}} = \dot{Q}_{23} = \dot{m} C_V (T_3 - T_2) \tag{1}$$

and the heat rejected by the working fluid during the process $4 \rightarrow 1$ is

$$\dot{Q}_{\text{out}} = \dot{Q}_{41} = \dot{m} C_P (T_4 - T_1). \tag{2}$$

The power output of the cycle can be written in the form,

$$\dot{W} = \dot{Q}_{\text{in}} - \dot{Q}_{\text{out}} = \dot{m} C_V \left[(T_3 - T_2) - k \left(T_4 - T_1 \right) \right] \tag{3}$$

and the thermal efficiency can be written as

$$\eta = 1 - \frac{\dot{Q}_{\text{out}}}{\dot{Q}_{\text{in}}} = 1 - \frac{k(T_4 - T_1)}{(T_3 - T_2)} \tag{4}$$

where $\dot{m}$ is the cycle mass times the number of cycles per second, C_V is the constant volume specific heat capacity, k is the ratio of the specific heat capacities (C_P / C_V),

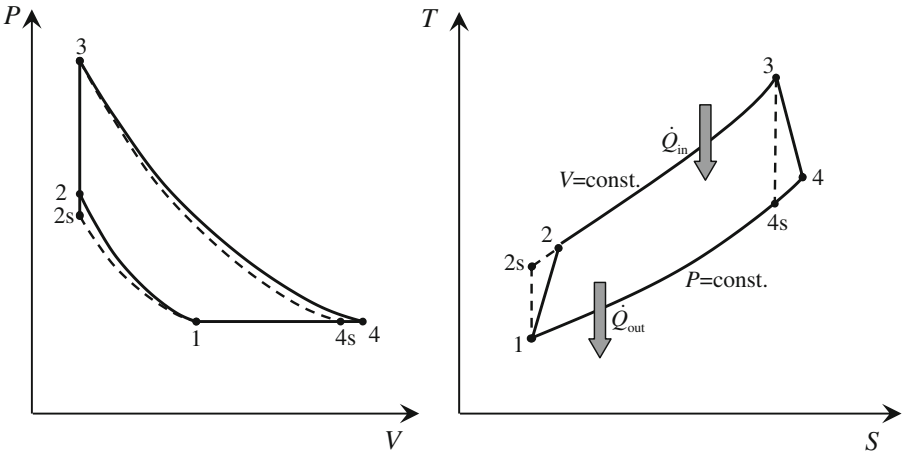

Fig. 1 *P-V* and *T-S* diagrams for the irreversible Atkinson cycle

and T_1, T_2, T_3, and T_4 are temperatures at states 1, 2, 3, and 4, respectively. From the 4–1 isobaric process, the maximum volume in the cycle, V_4, can be written as

$$V_4 = V_1(T_4/T_1). \tag{5}$$

The power density defined as the ratio of power output to the maximum volume in the cycle [21,22] then takes the form

$$\dot{W}_d = \dot{W}/V_4 = \frac{\dot{m}C_V}{V_1}\frac{[T_3 - T_2 - k(T_4 - T_1)]}{(T_4/T_1)}. \tag{6}$$

The second law of thermodynamics requires that

$$T_{2S}(T_{4S})^k = T_3(T_1)^k. \tag{7}$$

For the two adiabatic processes, the compression and expansion efficiencies [6]

$$\eta_C = \frac{T_{2S} - T_1}{T_2 - T_1} \tag{8}$$

and

$$\eta_E = \frac{T_3 - T_4}{T_3 - T_{4S}} \tag{9}$$

can be used to describe the irreversibility of the adiabatic processes. Using Eqs. 7, 8, and 9, we obtain

$$(T_2/T_1) = \frac{\eta_C + (\phi - 1)}{\eta_C} \tag{10}$$

and

$$(T_4/T_1) = \{\alpha - \eta_E[\alpha - (\alpha/\phi)^{1/k}]\} \tag{11}$$

where the cycle temperature ratio (α) and isentropic temperature ratio of the compression process (ϕ) are defined as

$$\alpha = T_3/T_1 \tag{12}$$

and

$$\phi = T_{2S}/T_1. \tag{13}$$

In terms of these parameters, it is easy to find the dimensionless power output, thermal efficiency, and dimensionless power density by substituting Eqs. 10 and 11 into Eqs. 3, 4, and 6, respectively, as

$$\overline{\dot{W}} = \frac{\dot{W}}{\dot{m}C_V T_1} = (\alpha - 1)(1 - k) - \frac{(\phi - 1)}{\eta_C} + k\eta_E \left[\alpha - (\alpha/\phi)^{1/k}\right], \quad (14)$$

$$\eta = 1 + \frac{k\eta_C \left\{(\alpha - 1) + \eta_E \left[(\alpha/\phi)^{1/k} - \alpha\right]\right\}}{[\eta_C(1 - \alpha) + (\phi - 1)]} \quad (15)$$

and

$$\overline{\dot{W}}_d = \frac{\dot{W}_d}{(\dot{m}C_V T_1/V_1)} = \frac{(\phi - 1) - \eta_C(\alpha + k - 1)}{\eta_C \left\{\alpha(\eta_E - 1) - \eta_E(\alpha/\phi)^{1/k}\right\}} - k. \quad (16)$$

One can maximize the power output given in Eq. 14 with respect to the isentropic temperature ratio of the compression process, ϕ, and can find it as

$$\phi_{mp} = (\eta_C \eta_E \alpha^{1/k})^{ak}. \quad (17)$$

The dimensionless MP output and the thermal efficiency at MP now can be found by substituting Eq. 17 into Eqs. 14 and 15, respectively, as

$$\overline{\dot{W}}_{max} = (\alpha - 1)(1 - k) - \frac{\{\left(\eta_C \eta_E \alpha^{1/k}\right)^{ak} - 1\}}{\eta_C} + k\eta_E \left[\alpha - (\alpha/\eta_C\eta_E)^a\right], \quad (18)$$

and

$$\eta_{mp} = 1 + \frac{k\eta_C \left\{(\alpha - 1) + \eta_E \left[(\alpha/\eta_C\eta_E)^a - \alpha\right]\right\}}{[\eta_C(1 - \alpha) + \{\left(\eta_C \eta_E \alpha^{1/k}\right)^{ak} - 1\}]} \quad (19)$$

where $a = 1/(k + 1)$ defined for simplicity. It is also possible to find the optimum isentropic temperature ratio of the compression process at MPD (ϕ_{mpd}) by differentiating with respect to ϕ and seeking a MPD, $\dot{W}_{d,max}$, by setting

$$\frac{\partial \overline{\dot{W}}_d}{\partial \phi} = \frac{k\alpha\phi_{mpd}(\eta_E - 1) - A}{k\eta_C\phi_{mpd}B^2} = 0 \quad (20)$$

where

$$A = \eta_E \left\{\phi_{mpd}(k + 1) - \eta_C(\alpha + k - 1) - 1\right\} (\alpha/\phi_{mpd})^{1/k} \quad (21)$$

and

$$B = \left\{\alpha(1 - \eta_E) + \eta_E(\alpha/\phi_{mpd})^{1/k}\right\}. \quad (22)$$

The maximum dimensionless power density $\overline{\dot{W}}_{\mathrm{d,max}}$ and the thermal efficiency at the MPD condition, which occurs at $\phi = \phi_{\mathrm{mpd}}$, can be written, respectively, as

$$\overline{\dot{W}}_{\mathrm{d,max}} = \frac{(\phi_{\mathrm{mpd}} - 1) - \eta_{\mathrm{C}}(\alpha + k - 1)}{\eta_{\mathrm{C}}\left\{\alpha(\eta_{\mathrm{E}} - 1) - \eta_{\mathrm{E}}(\alpha/\phi_{\mathrm{mpd}})^{1/k}\right\}} - k \tag{23}$$

and

$$\eta_{\mathrm{mpd}} = 1 + \frac{k\eta_{\mathrm{C}}\left\{(\alpha - 1) + \eta_{\mathrm{E}}\left[\left(\alpha/\phi_{\mathrm{mpd}}\right)^{1/k} - \alpha\right]\right\}}{\left[\eta_{\mathrm{C}}(1 - \alpha) + (\phi_{\mathrm{mpd}} - 1)\right]}. \tag{24}$$

3 Results and Discussion

In terms of power, power density, and thermal efficiency, a performance analysis has been carried out in order to investigate the performance of an irreversible Atkinson cycle. In the calculation, the k parameter is chosen as equal to 1.4, and also the curves a, b, and c of Figs. 2, 3, 4 correspond to the cases of $\eta_{\mathrm{C}} = \eta_{\mathrm{E}} = 0.90$, 0.95, and 1, respectively. Figures 2, 3, and 4 show the variations of the dimensionless power output ($\overline{\dot{W}} = \dot{W}/\dot{m}C_V T_1$), dimensionless power density ($\overline{\dot{W}}_{\mathrm{d}} = \dot{W}_{\mathrm{d}} V_1/\dot{m}C_V T_1$) and thermal efficiency (η) with isentropic temperature ratio of the compression process (ϕ) for various cycle temperature ratio (α) and internal irreversibilities (η_{C}, η_{E}). It is seen that $\overline{\dot{W}} - \phi$, $\overline{\dot{W}}_{\mathrm{d}} - \phi$, and $\eta - \phi$ characteristics are parabolic-like curves, and these curves shift right as α and η_{C}, η_{E} increase. For $\alpha = 5$ and $\eta_{\mathrm{C}} = \eta_{\mathrm{E}} = 0.95$, the comparisons

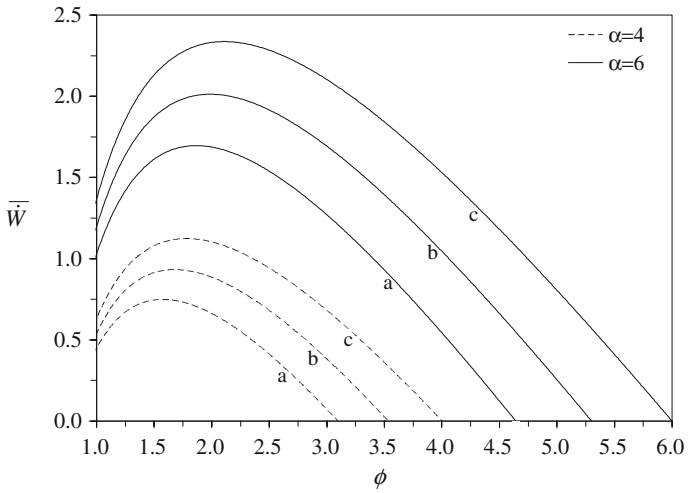

Fig. 2 Variation of the dimensionless power output with respect to the isentropic temperature ratio of the compression process for the parameter $k = 1.4$. Curves a, b, and c correspond to the cases of $\eta_{\mathrm{C}} = \eta_{\mathrm{E}} = 0.90$, 0.95, and 1, respectively

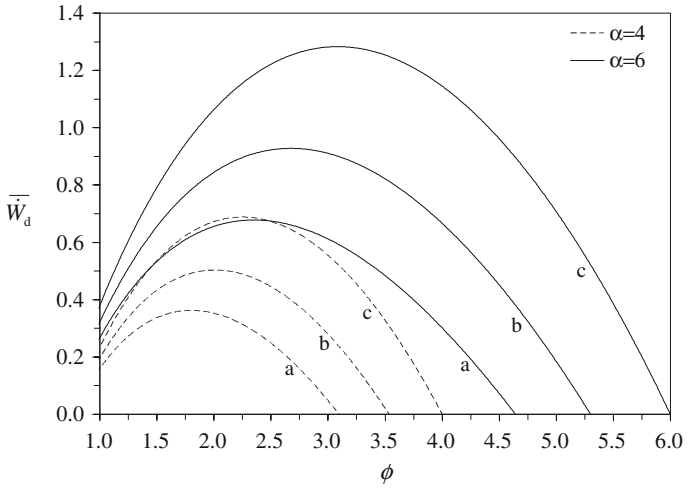

Fig. 3 Variation of the dimensionless power density with respect to the isentropic temperature ratio of the compression process for the parameter $k = 1.4$. Curves a, b, and c correspond to the cases of $\eta_C = \eta_E = 0.90, 0.95$, and 1, respectively

of several objective functions, namely, the dimensionless power output, dimensionless power density, and thermal efficiency with respect to the isentropic temperature ratio of the compression process, ϕ, are demonstrated in Fig. 5. It is seen from Fig. 5 that the optimum ϕ at the η_{max} conditions (ϕ_{mef}) is always greater than those at $\dot{W}_{max}$ and $\dot{W}_{d,max}$ conditions (ϕ_{mp}, ϕ_{mpd}), so we can write $\phi_{mef} > \phi_{mpd} > \phi_{mp}$. In the figure, points A, C, and E represent the maximum points at $\dot{W}_{max}$, $\dot{W}_{d,max}$, and η_{max} conditions, respectively. Points B and D are the thermal efficiencies at maximum $\dot{W}$ and $\dot{W}_d$ conditions. It is obvious from Fig. 5 that the optimal thermal efficiencies can symbolically be ordered as $\eta_{max} > \eta_{mpd} > \eta_{mp}$.

In Figs. 6 and 7, we plotted the variations of dimensionless power output and dimensionless power density with respect to the thermal efficiency for different selected values of the cycle temperature ratio (α) and isentropic efficiencies (η_C, η_E). From these figures, we can evaluate the effects of the design parameters on the power output, power density, and thermal efficiency for better performance. The curves in Figs. 6 and 7 are all in loop forms, and thus, they have two different maxima for both axes, which are $\overline{\dot{W}} - \eta$ and $\overline{\dot{W}}_d - \eta$, respectively. The performances in terms of $\dot{W}$, $\dot{W}_d$, and η decrease as α and $\eta_C = \eta_E$ decrease. Of course, the thermal efficiencies at MP output (η_{mp}) and MPD (η_{mpd}) conditions are lower than the maximum thermal efficiency (η_{max}). Moreover, the $\dot{W}$ and $\dot{W}_d$ at η_{max} conditions ($\dot{W}_{mef}$ and $\dot{W}_{d,mef}$) are lower than the $\dot{W}_{max}$ and $\dot{W}_{d,max}$. So we need to evaluate a compromise between the power-thermal efficiency and the power density-thermal efficiency. Also, we can observe from Figs. 6 and 7 that $\eta_{mp} - \eta_{max}$, or $\dot{W}_{max} - \dot{W}_{mef}$ and $\eta_{mpd} - \eta_{max}$, or $\dot{W}_{d,max} - \dot{W}_{mef}$ get closer to each other for decreasing α and $\eta_C = \eta_E$. By considering the power output, power density, and thermal efficiency of the heat engine together, the optimal design intervals in terms of $\dot{W} - \eta$ and $\dot{W}_d - \eta$ will be

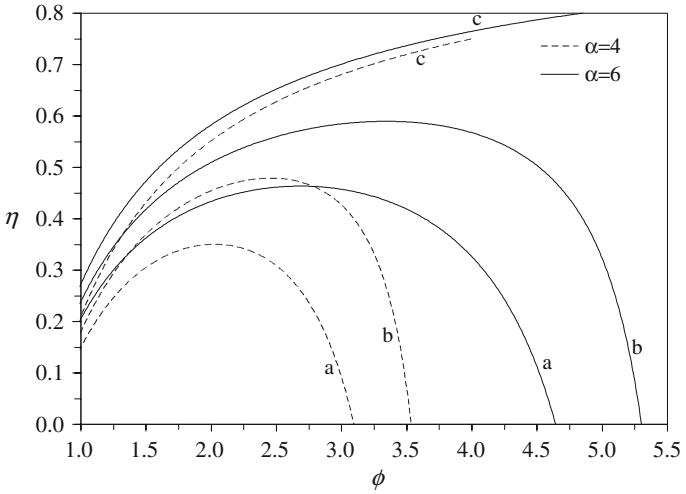

Fig. 4 Variation of the thermal efficiency with respect to the isentropic temperature ratio of the compression process for the parameter $k = 1.4$. Curves a, b, and c correspond to the cases of $\eta_C = \eta_E = 0.90$, 0.95, and 1, respectively

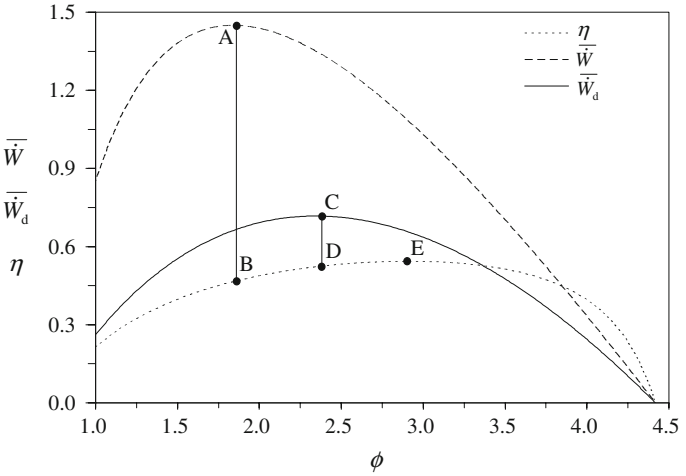

Fig. 5 Variations of the dimensionless power density, power output, and thermal efficiency with respect to the isentropic temperature ratio of the compression process for the parameters $\alpha = 5$, $\eta_C = \eta_E = 0.95$, and $k = 1.4$

$$\dot{W}_{\max} \geq \dot{W} \geq \dot{W}_{\text{mef}}, \quad \text{or} \quad \eta_{\text{mp}} \leq \eta \leq \eta_{\max} \tag{25}$$

and

$$\dot{W}_{\text{d,max}} \geq \dot{W}_{\text{d}} \geq \dot{W}_{\text{d,mef}}, \quad \text{or} \quad \eta_{\text{mpd}} \leq \eta \leq \eta_{\max}. \tag{26}$$

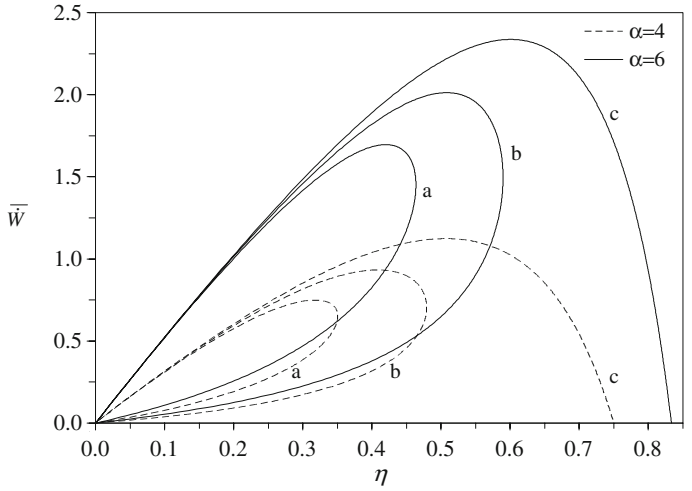

Fig. 6 Variation of the dimensionless power output with respect to the thermal efficiency for the parameter $k = 1.4$. Curves a, b, and c correspond to the cases of $\eta_C = \eta_E = 0.90$, 0.95, and 1, respectively

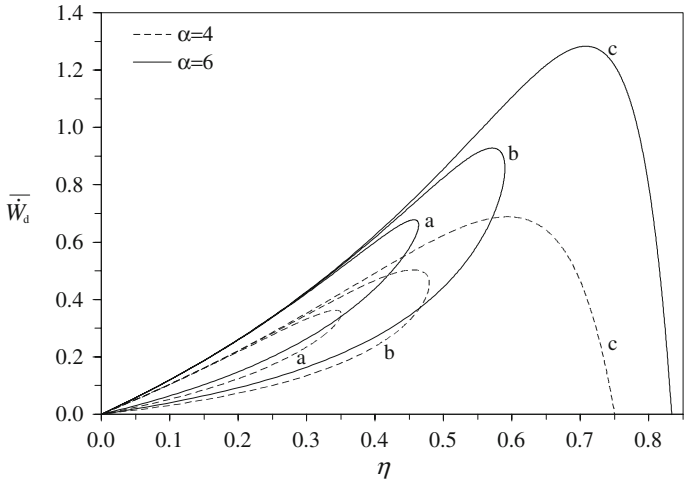

Fig. 7 Variation of the dimensionless power density with respect to the thermal efficiency for the parameter $k = 1.4$. Curves a, b, and c correspond to the cases of $\eta_C = \eta_E = 0.90$, 0.95, and 1, respectively

The effects of the α and $\eta_C = \eta_E$ on the optimal ϕ and optimal thermal efficiencies are shown in Figs. 8 and 9 at $\dot{W}_{max}$ and $\dot{W}_{d,max}$ conditions. The common characteristic of these figures is that the optimal isentropic temperature ratios of the compression process (ϕ_{mp} and ϕ_{mpd}) and the optimal thermal efficiencies (η_{mp} and η_{mpd}) all increase as α and $\eta_C = \eta_E$ increase. For specified α and $\eta_C = \eta_E$ values, the optimal ϕ and η values take different values according to the particular objective function, i.e., $\dot{W}_{max}$ and $\dot{W}_{d,max}$. To emphasize the differences, a numerical example is given: for $\alpha = 5$ and $\eta_C = \eta_E = 0.95$, $\phi_{mp} = 1.84$, and $\eta_{mp} = 0.465$ at $\dot{W}_{max}$ conditions

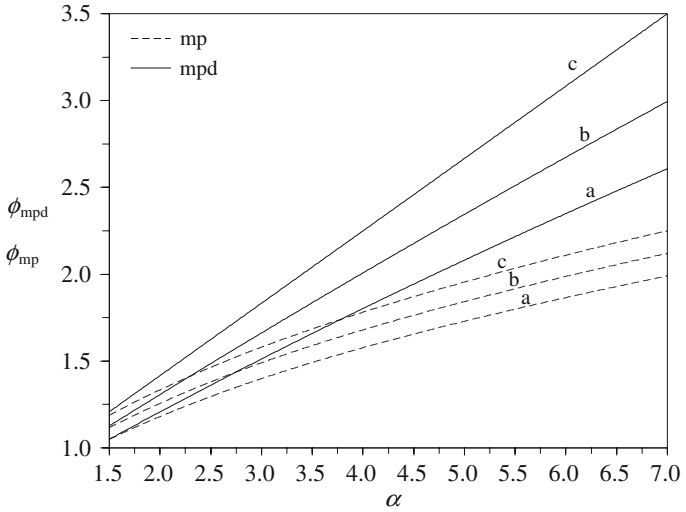

Fig. 8 Variations of the isentropic temperature ratios of the compression process at MPD and MP conditions with respect to the cycle temperature ratio for the parameter $k = 1.4$. Curves a, b, and c correspond to the cases of $\eta_C = \eta_E = 0.90$, 0.95, and 1, respectively

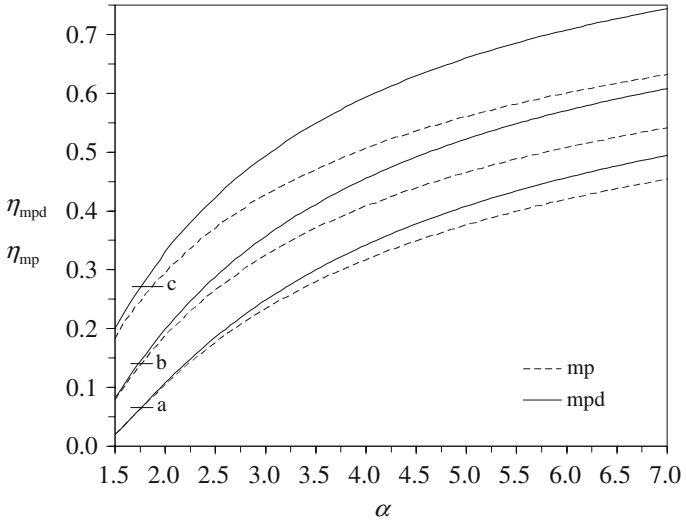

Fig. 9 Variations of the thermal efficiencies at MPD and MP conditions with respect to the cycle temperature ratio for the parameter $k = 1.4$. Curves a, b, and c correspond to the cases of $\eta_C = \eta_E = 0.90, 0.95$, and 1, respectively

and $\phi_{mpd} = 2.34$ and $\eta_{mpd} = 0.522$ at $\dot{W}_{d,max}$ conditions. It should be noted that the optimal design parameters differ according to the specified objective function. Therefore, it is important to consider this situation in design processes. Variations of the volume ratios (V_4/V_1) in the cycle with α for the MPD and MP conditions are shown in Fig. 10. An engine working at MPD is smaller than the one working at MP,

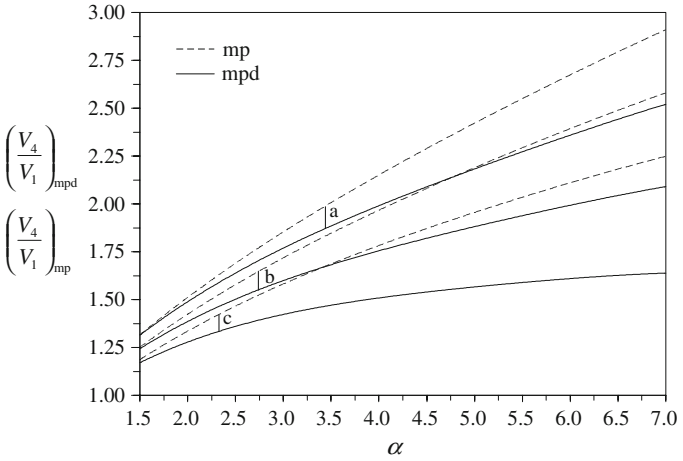

Fig. 10 Variations of the volume ratios at MPD and MP conditions with respect to the cycle temperature ratio for the parameter $k = 1.4$. Curves a, b, and c correspond to the cases of $\eta_C = \eta_E = 0.90$, 0.95, and 1, respectively

because its maximum volume is always smaller. An increase in the internal irreversibility parameter causes a decrease in the volume ratio. Another important point to notice in Fig. 10 is that the maximum volume at MPD increases more slowly than that at MP as α increases. The volume ratios in the cycle for the MPD and MP conditions are given by

$$(V_4/V_1)_{\mathrm{mpd}} = \{\alpha - \eta_E[\alpha - (\alpha/\phi_{\mathrm{mpd}})^{1/k}]\} \tag{27}$$

and

$$(V_4/V_1)_{\mathrm{mp}} = \left\{\alpha - \eta_E\left[\alpha - \frac{\alpha^{\left(\frac{k-1}{k^2}\right)}}{(\eta_C\eta_E)^{1/k}}\right]\right\}. \tag{28}$$

It can be concluded from the comparisons of performances at $\dot{W}_{d,\max}$ with respect to the $\dot{W}_{\max}$ condition that the optimal performance at $\dot{W}_{d,\max}$ over $\dot{W}_{\max}$ conditions provide significant advantages in terms of thermal efficiency and engine sizes.

4 Conclusions

A comparative performance analysis based on MPD and MP criteria has been performed for an irreversible Atkinson heat-engine model consisting of one constant volume heating branch, one constant pressure cooling branch, and two adiabatic branches with consideration of internal irreversibilities. In this perspective, the design parameters that maximize the power and power density of the irreversible Atkinson cycle have been investigated. The relations between the power and the isentropic temperature ratio of the compression process and between the power density and the isentropic

temperature ratio of the compression process and between the efficiency and the isentropic temperature ratio of the compression process of the cycle have been derived. The power versus isentropic temperature ratio of the compression process curves, the power density versus isentropic temperature ratio of the compression process curves, the efficiency versus isentropic temperature ratio of the compression process curves, the power versus efficiency curves, and the power density versus efficiency curves for the Atkinson cycle have been illustrated by numerical examples. The irreversibility in the adiabatic processes always reduces the power output, power density, and thermal efficiency. From the view points of engine size and thermal efficiency, the engine design based on MPD has the advantage of smaller size and higher efficiency when compared with one based on MP. The results presented in this analysis generalize the results of previous studies on this subject and may provide guidelines for determination of the optimal design and operating conditions of real heat engines.

References

1. Wikipedia: Atkinson cycle. Available via DIALOG. http://www.answers.com/topic/atkinson-cycle. Cited 15 Dec 2008
2. B. Andresen, R.S. Berry, M.J. Ondrechen, P. Salamon, Acc. Chem. Res. **17**, 266 (1984)
3. S. Sieniutycz, J.S. Shiner, J. Non-Equilib. Thermodyn. **19**, 303 (1994)
4. A. Bejan, J. Appl. Phys. **79**, 1191 (1996)
5. R.S. Berry, V.A. Kazakov, S. Sieniutycz, Z. Szwast, A.M. Tsirlin, *Thermodynamic Optimization of Finite Time Processes* (Wiley, Chichester, 1999)
6. L. Chen, C. Wu, F. Sun, J. Non-Equilib. Thermodyn. **24**, 327 (1999)
7. A. Durmayaz, O.S. Sogut, B. Sahin, H. Yavuz, Prog. Energ. Combust. Sci. **30**, 175 (2004)
8. H.S. Leff, Am. J. Phys. **55**, 602 (1987)
9. A. Al-Sarkhi, B.A. Akash, Int. Commun. Heat Mass Trans. **29**, 1159 (2002)
10. Y. Ge, L. Chen, F. Sun, C. Wu, Appl. Energ. **81**, 397 (2005)
11. K. Kamiuto, Appl. Energ. **83**, 583 (2006)
12. Y. Zhao, J. Chen, Appl. Energ. **83**, 789 (2006)
13. Y. Ge, L. Chen, F. Sun, C. Wu, Appl. Energ. **83**, 1210 (2006)
14. Y. Ge, L. Chen, F. Sun, C. Wu, J. Energ. Ins. **80**, 52 (2007)
15. L. Chen, W.L. Zhang, F. Sun, Appl. Energ. **84**, 512 (2007)
16. S.S. Hou, Energ. Convers. Manage. **48**, 1683 (2007)
17. Y.R. Zhao, J. Chen, Appl. Therm. Eng. **27**, 2051 (2007)
18. J.C. Lin, S.S. Hou, Appl. Energ. **84**, 904 (2007)
19. L. Chen, Y. Ge, F. Sun, Proc. Inst. Mech. Eng.: Part D.-J. Autom. Eng. **222**, 1489 (2008)
20. J.A. Caton, J. Eng. Gas Turb. Power-Trans. ASME **130**, (2008)
21. B. Sahin, A. Kodal, H. Yavuz, J. Phys. D: Appl. Phys. **28**, 1309 (1995)
22. B. Sahin, A. Kodal, T. Yilmaz, H. Yavuz, J. Phys. D: Appl. Phys. **29**, 1162 (1996)
23. B. Sahin, A. Kodal, H. Yavuz, Energy **21**, 1219 (1996)
24. B. Sahin, A. Kodal, H. Yavuz, J. Phys. D: Appl. Phys. **29**, 1473 (1996)
25. A. Medina, J.M.M. Roco, A.C. Hernandez, J. Phys. D: Appl. Phys. **29**, 2802 (1996)
26. B. Sahin, A. Kodal, S.S. Kaya, J. Phys. D: Appl. Phys. **31**, 2125 (1998)
27. A. Kodal, J. Phys. D: Appl. Phys. **32**, 2958 (1999)
28. A. Kodal, B. Sahin, T. Yilmaz, Energ. Convers. Manage. **41**, 235 (2000)
29. L. Chen, J. Zheng, F. Sun, C. Wu, J. Phys. D: Appl. Phys. **34**, 422 (2001)
30. L. Chen, J. Zheng, F. Sun, C.Wu, Open Syst. Info. Dyn. **8**, 241 (2001)
31. L. Chen, J. Zheng, F. Sun, C.Wu, Phys. Scripta **64**, 184 (2001)
32. L. Chen, J. Zheng, F. Sun, C. Wu, Energ. Convers. Manage. **43**, 33 (2002)
33. B. Sahin, U. Kesgin, A. Kodal, N. Vardar, Energ. Convers. Manage. **43**, 2019 (2002)
34. L. Chen, J. Lin, F. Sun, C. Wu, Energ. Convers. Manage. **39**, 337 (1998)
35. P.Y. Wang, S.S. Hou, Energ. Convers. Manage. **46**, 2637 (2005)